

# Electrochemical Oxidation of Ferrocene: A Strong Dependence on the Concentration of the Supporting Electrolyte for Nonpolar Solvents

Duoduo Bao, Brent Millare, Wei Xia, Benjamin G. Steyer, Alexander A. Gerasimenko, Amy Ferreira, Antonio Contreras, and Valentine I. Vullev\*

Department of Bioengineering, University of California, Riverside, California 92521

Received: October 14, 2008; Revised Manuscript Received: December 4, 2008

The estimation of the driving force for photoinduced charge-transfer processes, using the Rehm–Weller equation, requires the employment of redox and spectroscopic quantities describing the participating electron donor and acceptor. Although the spectroscopic data are usually obtained from diluted solutions, the redox potentials are most frequently obtained from electrochemical measurements conducted in concentrated electrolyte solutions. To correct for the differences in the media, in which the various types of measurements are conducted, a term, based on the Born equation for solvation energy of ions, is introduced in the Rehm–Weller equation. The Born correction term, however, requires a prior knowledge of the dielectric constants of the electrolyte solutions used for the redox measurements. Because of limited information for such dielectrics, the values for the dielectric constants of electrolyte solutions are approximated to the values of the dielectric constants of the corresponding neat solvents. We examined the validity of this approximation. Using cyclic voltammetry, we recorded the first one-electron oxidation potential of ferrocene for three different solvents in the presence of 1–500 mM supporting electrolyte. The dielectric constants for some of the electrolyte solutions were extracted from fluorescence measurements of a dimethylaminonaphthalimide chromophore that exhibits pronounced solvatochromism. The dielectric constants of the concentrated electrolyte solutions correlated well with the corresponding oxidation potentials. The dependence of the oxidation potential of ferrocene on the electrolyte concentration for different solvents revealed that the abovementioned approximation in the Born correction term indeed introduces a significant error in the estimation of the charge-transfer driving force from redox data collected using relatively nonpolar solvents.

## Introduction

This article describes electrochemical investigation of the redox properties of ferrocene in the presence of various concentrations of a supporting electrolyte for different organic solvent media. We observed shifts of up to 0.5 V in the oxidation potential of ferrocene with an increase in the electrolyte concentration to 500 mM.

The Rehm–Weller equation provides an important relation, involving measurable quantities, that allows for estimation of the driving force (i.e., the change in the Gibbs energy,  $\Delta G_{\text{et}}^{(0)}$ ) of photoinduced electron transfer processes:<sup>1–3</sup>

$$\Delta G_{\text{et}}^{(0)} = F(E_{\text{D}^{\text{z}_\text{D}}/\text{D}^{\text{z}_\text{D}}}^{(0)} - E_{\text{A}^{\text{z}_\text{A}}/\text{A}^{\text{z}_\text{A}-n}}^{(0)}) - \mathcal{C}_{00} + \Delta G_{\text{S}} + W \quad (1)$$

where  $E_{\text{D}^{\text{z}_\text{D}}/\text{D}^{\text{z}_\text{D}}}^{(0)}$  and  $E_{\text{A}^{\text{z}_\text{A}}/\text{A}^{\text{z}_\text{A}-n}}^{(0)}$  are the standard oxidation and reduction potentials for the donor and the acceptor, respectively;  $F$  is the Faraday constant;  $\mathcal{C}_{00}$  is the zero-to-zero energy of the principal chromophore; and  $\Delta G_{\text{S}}$  and  $W$  are the Born and Coulombic correction terms, respectively,

$$\Delta G_{\text{S}} = \frac{nq^2}{8\pi\epsilon_0} \left( \frac{2z_{\text{D}} + n}{r_{\text{D}}} \left( \frac{1}{\epsilon} - \frac{1}{\epsilon_{\text{D}}} \right) - \frac{2z_{\text{A}} - n}{r_{\text{A}}} \left( \frac{1}{\epsilon} - \frac{1}{\epsilon_{\text{A}}} \right) \right) \quad (2)$$

$$W = \frac{n(z_{\text{A}} - z_{\text{D}} - n)q^2}{4\pi\epsilon_0\epsilon R_{\text{DA}}} \quad (3)$$

where  $r_{\text{D}}$  and  $r_{\text{A}}$  are the donor and acceptor radii, respectively;  $R_{\text{DA}}$  is the center-to-center donor acceptor distance;  $n$  is the

number of transferred electrons;  $q$  is an elementary charge;  $z_{\text{D}}$  and  $z_{\text{A}}$  are the charges of the donor and the acceptor, respectively, prior to the electron-transfer process; and  $\epsilon_0$  is the electric permittivity of vacuum.

In eq 2, although  $\epsilon_{\text{D}}$  and  $\epsilon_{\text{A}}$  are the dielectric constants of the solutions in which the redox potentials of the donor and the acceptor, respectively, are measured,  $\epsilon$  is the dielectric constant of the media, for which  $\Delta G_{\text{et}}^{(0)}$  is calculated and the spectroscopic measurements for estimation of  $\mathcal{C}_{00}$  are conducted. The Born term, therefore, introduces a correction for the differences in the solvation energies for the charged species,<sup>4,5</sup> involved in the electron-transfer process, when in media with dielectric constants  $\epsilon$ ,  $\epsilon_{\text{D}}$ , and  $\epsilon_{\text{A}}$ ; i.e.,  $\Delta G_{\text{S}}/F$  corrects the values of the redox potentials,  $E_{\text{D}^{\text{z}_\text{D}}/\text{D}^{\text{z}_\text{D}}}^{(0)}$  and  $E_{\text{A}^{\text{z}_\text{A}}/\text{A}^{\text{z}_\text{A}-n}}^{(0)}$ , measured in media with dielectric constants  $\epsilon_{\text{D}}$  and  $\epsilon_{\text{A}}$  to the expected values for  $E_{\text{D}^{\text{z}_\text{D}}/\text{D}^{\text{z}_\text{D}}}^{(0)}$  and  $E_{\text{A}^{\text{z}_\text{A}}/\text{A}^{\text{z}_\text{A}-n}}^{(0)}$ , if they were measured in media with dielectric constant  $\epsilon$ .

The redox potentials,  $E_{\text{D}^{\text{z}_\text{D}}/\text{D}^{\text{z}_\text{D}}}^{(0)}$  and  $E_{\text{A}^{\text{z}_\text{A}}/\text{A}^{\text{z}_\text{A}-n}}^{(0)}$ , are most frequently obtained from electrochemical measurements, which are conducted in concentrated electrolyte solutions. Because data for dielectric properties of electrolyte solutions are scarce,  $\epsilon_{\text{D}}$  and  $\epsilon_{\text{A}}$  are approximated with the dielectric constants of the corresponding neat solvents.<sup>2,6,7</sup> This approximation, although broadly employed, can be a source of a significant error in the estimation of  $\Delta G_{\text{et}}^{(0)}$ .

Assuming that  $\epsilon^{-1} \gg \epsilon_{\text{D}}^{-1}$  and  $\epsilon^{-1} \gg \epsilon_{\text{A}}^{-1}$  allows for an alternative approximation for the Born term in eq 2 that for a one-electron transfer ( $n = 1$ ) between noncharged donor and acceptor is  $\Delta G_{\text{S}} \approx q^2(r_{\text{D}}^{-1} + r_{\text{A}}^{-1})(8\pi\epsilon_0\epsilon)^{-1}$ .<sup>8</sup> This alternative

\* To whom correspondence should be addressed. E-mail: vullev@ucr.edu.

approximation, however, is not universally applicable: it is acceptable solely for charge-transfer studies in relatively non-polar media, for which the redox potentials are determined in relatively polar solvents in the presence of high electrolyte concentration.

Due to the robustness of its reversibility at experimentally accessible potentials, the ferrocenium/ferrocene redox couple,  $\text{Fc}^+/\text{Fc}$  ( $\text{Fc} = \text{Fe}(\text{C}_5\text{H}_5)_2$ ), has been established as one of the standards for calibration of electrochemical measurements and extensively investigated.<sup>9–13</sup> The oxidation potential of ferrocene,  $E_{\text{Fc}^+/\text{Fc}}^{(0)}$ , recorded in the presence of  $\sim 0.1$  M supporting electrolyte, manifests a relatively small dependence on the polarity of the neat solvent used for the measurements.<sup>11,14,15</sup> Furthermore,  $E_{\text{Fc}^+/\text{Fc}}^{(0)}$  shows negligible dependence on the chemical composition of the electrolyte and the material of the working electrode used for the voltammetric measurements.<sup>16</sup> Changes in the concentration of the supporting electrolyte, however, cause dramatic shifts in the oxidation potential of ferrocene for dilute solutions.<sup>17–19</sup> These redox properties, which are not limited to ferrocene only, raise questions about the feasibility of the approximation of  $\epsilon_{\text{D}}$  and  $\epsilon_{\text{A}}$  (eq 2) to the dielectric constants of the corresponding neat solvents.

Herein, we examine the errors that can be potentially introduced in the Born correction term through the abovementioned approximation of  $\epsilon_{\text{D}}$  and  $\epsilon_{\text{A}}$ . We describe a relatively facile approach for estimation of redox potentials for neat solvent media and hence, obtaining the exact, rather than approximate, values for  $\Delta G_{\text{S}}$ .

Using cyclic voltammetry (CV), we investigated the changes in the oxidation potential of ferrocene in the presence of various concentrations of tetrabutylammonium tetrafluoroborate (TBA-TFB) as a supporting electrolyte for three aprotic organic solvents broadly used for electrochemical measurements: dichloromethane ( $\text{CH}_2\text{Cl}_2$ ), acetonitrile (MeCN) and *N,N*-dimethylformamide (DMF). An increase in the electrolyte concentration shifts the oxidation potential of Fc to values more negative by as much as 0.5 V.

Using the solvatochromic properties of a dimethylaminonaphthalimide fluorophore, we estimated the dielectric constants of  $\text{CH}_2\text{Cl}_2$  solutions of TBATFB with different concentrations. An increase in the electrolyte concentration to 500 mM resulted in a 2.7-fold increase in the dielectric constant of the solution in comparison with the dielectric constant of the neat solvent,  $\text{CH}_2\text{Cl}_2$ . The observed shifts in the oxidation potential of Fc correlated well with the dielectric properties of the electrolyte solution for electrolyte concentration exceeding  $\sim 20$  mM.

## Results and Discussion

**Redox Properties of Ferrocene.** For this series of studies, we chose ferrocene as a redox probe because of its well-defined one-electron oxidation to a ferrocenium ion,  $\text{Fc}^+$ .<sup>11</sup> Due to the relative stability of  $\text{Fc}^+$ , ferrocene exhibits reversible oxidation behavior in voltammetry measurements.<sup>14</sup> Its oxidation potential,  $E_{\text{Fc}^+/\text{Fc}}^{(0)}$ , therefore, can be reliably approximated to its half-wave potential,  $E_{\text{Fc}^+/\text{Fc}}^{(1/2)}$ ,<sup>14,16</sup> defined as the midpoint between the values of the potentials corresponding to the anodic and the cathodic peak in the cyclic voltammograms of Fc. We selected three organic solvents,  $\text{CH}_2\text{Cl}_2$ , MeCN, and DMF, which are electrochemically inert within the window of potentials used for this study.

For each of the solvent media, an increase in the concentration of the electrolyte from 1 to 500 mM resulted in considerable shifts of the anodic peaks to less positive values (Figure 1).

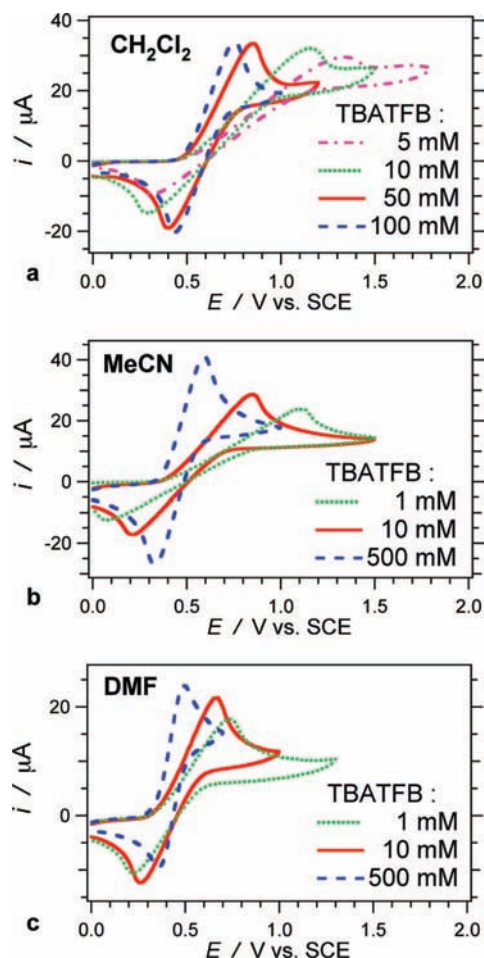


**Figure 1.** Cyclic voltammograms of ferrocene (5 mM) in the presence of various concentrations of the supporting electrolyte, TBATFB, for different solvents: (a) dichloromethane, (b) acetonitrile, and (c) dimethylformamide (scan rates = 50 mV/s).

The cathodic peaks concurrently shifted to a lesser extent toward more positive values. As a result, for all three solvent media, the increase in the TBATFB concentration shifted the oxidation potential of Fc,  $E_{\text{Fc}^+/\text{Fc}}^{(1/2)}$ , toward more negative values (Figure 2 and Table 1). This electrolyte-induced effect was most pronounced for the least-polar of the three solvents,  $\text{CH}_2\text{Cl}_2$ .

Upon the increase in the electrolyte concentration, the oxidation potentials of Fc for the three solvents asymptotically approached values that are within 0.1 from one another (Figure 2); that is,  $E_{\text{Fc}^+/\text{Fc}}^{(1/2)}$  ( $C_{\text{TBATFB}} \rightarrow \infty$ ) is equal to 0.52, 0.44, and 0.43 V vs SCE for  $\text{CH}_2\text{Cl}_2$ , MeCN, and DMF, respectively. The increase in the electrolyte concentration increases the dielectric constant and, hence, decreases the inverse values of the dielectric constants,  $\epsilon^{-1}$ , of the solutions. (For the Born term in eq 1, it is the values of the inverse dielectric constants,  $\epsilon^{-1}$ , that are important.) Therefore, for relatively large electrolyte concentrations, the absolute differences between the small values of  $\epsilon^{-1}$  are relatively small, resulting in small differences in  $E_{\text{Fc}^+/\text{Fc}}^{(1/2)}$ .

**Dielectric Properties of  $\text{CH}_2\text{Cl}_2$  Electrolyte Solutions.** We used *N*-phenyl-4-dimethylamino-1,8-naphthalimide (Ph-ANI) for estimating the dielectric constants of the  $\text{CH}_2\text{Cl}_2$  solutions of TBATFB. The lowest excited state of Ph-ANI has a charge-transfer character. An increase in the media polarity, therefore, causes a red shift in the fluorescence spectrum of Ph-ANI (Figure 3). This solvatochromism appeared most pronouncedly for solvents with relatively low medium polarity. For example,

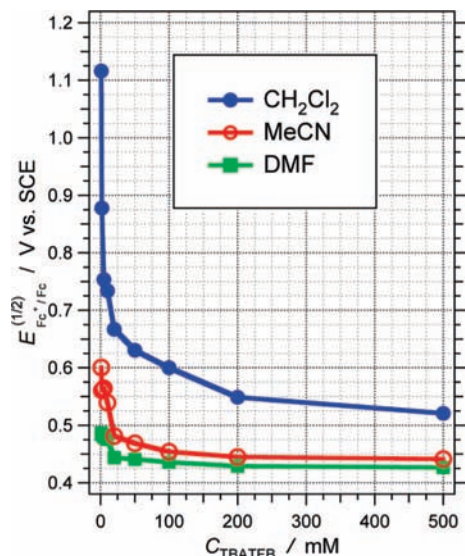


**Figure 2.** Dependence of the half-wave oxidation potential of ferrocene,  $E_{\text{Fc}^{+}/\text{Fc}}^{(1/2)}$ , on the concentration of the supporting electrolyte,  $C_{\text{TBATFB}}$ , for three different solvents.

**TABLE 1: Half-Wave Oxidation Potentials of Ferrocene,  $E_{\text{Fc}^{+}/\text{Fc}}^{(1/2)}$ , for Different Solvents in the Presence of Various Concentrations of TBATFB<sup>a</sup>**

$C_{\text{TBATFB}} / \text{mM}$	solvent		
	$\text{CH}_2\text{Cl}_2$	MeCN	DMF
1	$1.12 \pm 0.02$	$0.600 \pm 0.008$	$0.487 \pm 0.006$
2	$0.878 \pm 0.029$	$0.561 \pm 0.002$	$0.484 \pm 0.004$
5	$0.754 \pm 0.016$	$0.564 \pm 0.003$	$0.479 \pm 0.001$
10	$0.734 \pm 0.006$	$0.539 \pm 0.007$	$0.476 \pm 0.010$
20	$0.667 \pm 0.001$	$0.481 \pm 0.002$	$0.444 \pm 0.001$
50	$0.630 \pm 0.004$	$0.469 \pm 0.002$	$0.441 \pm 0.002$
100	$0.600 \pm 0.003$	$0.454 \pm 0.006$	$0.436 \pm 0.004$
200	$0.549 \pm 0.006$	$0.445 \pm 0.005$	$0.429 \pm 0.003$
500	$0.521 \pm 0.004$	$0.441 \pm 0.003$	$0.427 \pm 0.002$

<sup>a</sup> The oxidation potentials are reported in volts vs SCE.

as the media changed from  $\text{CH}_2\text{Cl}_2$  ( $\epsilon = 8.93$ ) to benzonitrile (PhCN,  $\epsilon = 25.9$ ), the maximum of the fluorescence spectrum of Ph-ANI shifted almost 13 nm to the red.

The increase in the concentration of the electrolyte in  $\text{CH}_2\text{Cl}_2$  caused a similar red shift in the fluorescence spectrum of Ph-ANI (Figure 4). Relating the spectral maxima for the electrolyte solutions (Figure 4b and c) with the spectral maxima for organic solvents with known dielectric constants (Figure 3b) allowed us to extract the dielectric constants of the  $\text{CH}_2\text{Cl}_2$  solutions with various concentrations of TBATFB (Figure 5 and Table 2).

The increase in the electrolyte concentration caused close to a 3-fold increase in the dielectric constant of the  $\text{CH}_2\text{Cl}_2$  solutions. Although for neat  $\text{CH}_2\text{Cl}_2$ ,  $\epsilon^{-1} = 0.11$ , for 500 mM TBATFB solution in  $\text{CH}_2\text{Cl}_2$ ,  $\epsilon^{-1} = 0.041$ . For ferrocene, the Born correction term (eq 2) translated this difference in  $\epsilon^{-1}$  into a difference of about 0.2 V between  $E_{\text{Fc}^{+}/\text{Fc}}^{(1/2)}$  for the neat solvent and for the electrolyte solution. This finding indicates that for this particular solvent system, approximating  $\epsilon_D$  (or  $\epsilon_A$ ) to the dielectric constant of the neat organic solvent,  $\text{CH}_2\text{Cl}_2$ , introduces a nontrivial error.

**Correlation between Oxidation Potential and Dielectric Constant.** The oxidation potential of ferrocene,  $E_{\text{Fc}^{+}/\text{Fc}}^{(1/2)}$ , and the dielectric constant of the electrolyte solutions manifested similar trends in their dependence on the concentration of TBATFB (Figures 2 and 5).

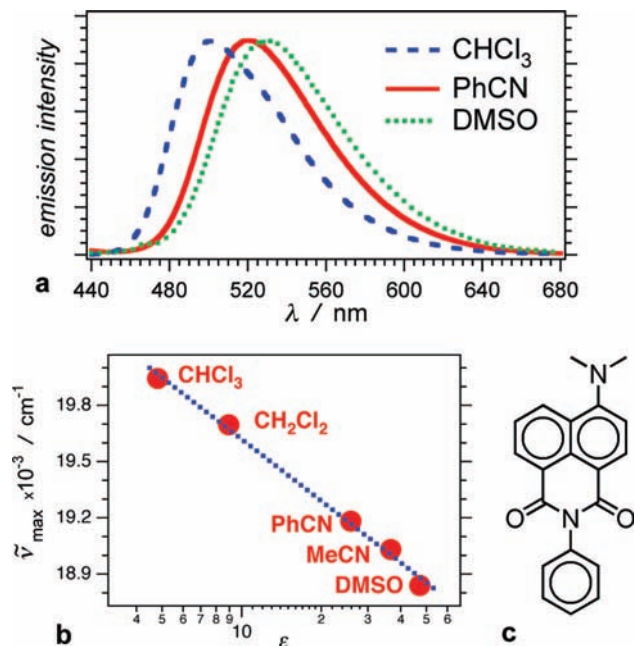


**Figure 3.** Solvatochromism of Ph-ANI. (a) Fluorescence spectra of Ph-ANI for different solvents (10  $\mu\text{M}$  Ph-ANI,  $\lambda_{\text{ex}} = 410$  nm, intensities normalized at  $\lambda_{\text{em}}^{\text{max}}$ ). (b) Dependence of the fluorescence maximum on the dielectric constant of the solvent:  $\text{CHCl}_3$ ,  $\text{CH}_2\text{Cl}_2$ , PhCN, MeCN, and DMSO. (c) Structural chemical formula of Ph-ANI.

As predicted by the Born equation,  $E_{\text{Fc}^{+}/\text{Fc}}^{(1/2)}$  should manifest linear dependence on the inverse dielectric constant of the media,  $\epsilon^{-1}$ , and the slope of  $E_{\text{Fc}^{+}/\text{Fc}}^{(1/2)}$  vs  $\epsilon^{-1}$  should be equal to  $q/(8\pi\epsilon_0 r_{\text{Fc}})$ .<sup>5</sup> An examination of the correlation between  $E_{\text{Fc}^{+}/\text{Fc}}^{(1/2)}$  and  $\epsilon^{-1}$  for  $\text{CH}_2\text{Cl}_2$  electrolyte media showed two distinct regions (Figure 6). For electrolyte concentrations exceeding 20 mM, the slope of the linear fit yielded a value of 2.6 Å for the radius of ferrocene,  $r_{\text{Fc}}$ . For electrolyte concentrations smaller than 5 mM, on the other hand, the linear fit produced an unrealistically small value for  $r_{\text{Fc}}$ . Employment of media with relatively large electrolyte concentration (e.g.,  $C_{\text{TBATFB}} \geq 20$  mM) for electrochemical measurements therefore assures reliable determination of  $E_{\text{Fc}^{+}/\text{Fc}}^{(1/2)}$ .

Despite the good correlation between  $E_{\text{Fc}^{+}/\text{Fc}}^{(1/2)}$  and  $\epsilon^{-1}$  for the  $\text{CH}_2\text{Cl}_2$  electrolyte solutions (for  $C_{\text{TBATFB}} \geq 20$  mM), these results should be approached with caution. The fluorescence solvatochromism of Ph-ANI allowed us to determine the bulk dielectric constant of the electrolyte  $\text{CH}_2\text{Cl}_2$  solutions. The electrochemical oxidation, on the other hand, is an interfacial process. At the surface of the working electrode, the electrolyte concentration differs from the bulk concentration of the supporting electrolyte. Furthermore, the adsorbed redox species, Fc, are not surrounded only by the electrolyte solution; they are also in contact with the electrode material. Therefore, the dielectric constant of the microenvironment of the ferrocene species, upon their oxidation at the electrode surface, is different from the dielectric constant of the bulk solution determined from the fluorescence measurements. For the described system, however, this difference did not compromise the quality of the correlation between the oxidation potential and the inverse values of the bulk dielectric constant.

**Redox Behavior of Fc in Dilute Electrolyte Solutions.** A decrease in the electrolyte concentration below  $\sim 10$  mM caused a sharp shift of  $E_{\text{Fc}^{+}/\text{Fc}}^{(1/2)}$  toward more positive values for all three solvent media (Figure 2). As a result, a linear correlation analysis based on the Born equation yielded an abnormally small value for  $r_{\text{Fc}}$  for diluted electrolyte solutions (Figure 6).

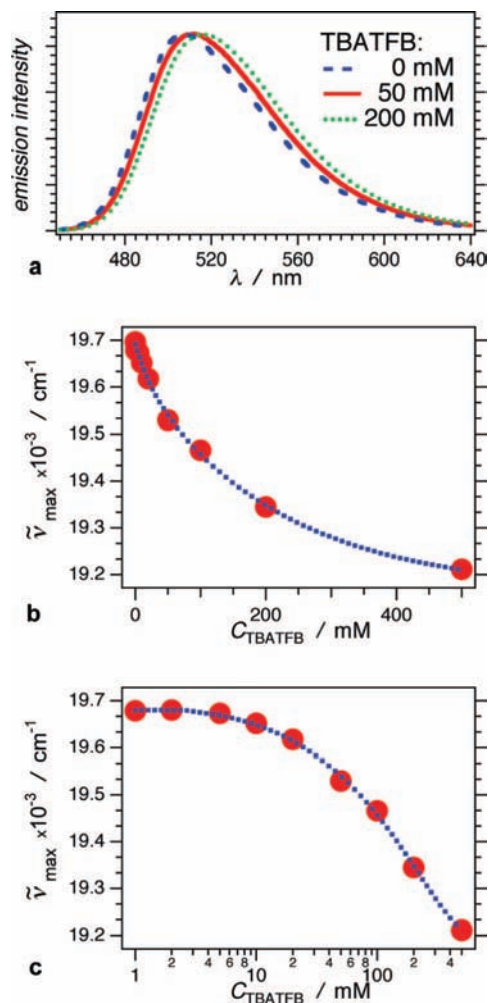


**Figure 4.** Fluorescence properties of Ph-ANI for dichloromethane with various concentrations of electrolyte, TBATFB. (a) Fluorescence spectra of Ph-ANI in the presence of various concentrations of TBATFB (10  $\mu$ M Ph-ANI,  $\lambda_{\text{ex}} = 410$  nm, intensities normalized at  $\lambda_{\text{fl}}^{\text{max}}$ ). (b, c) Dependence of the fluorescence maximum on the electrolyte concentration,  $C_{\text{TBATFB}}$ , presented (b) linearly and (c) logarithmically. The dotted lines represent an exponential fit of the fluorescence maximum vs the TBATFB concentration.

The concentration of ferrocene for the described CV measurements was 5 mM. As the electrolyte concentration decreases to the lower millimolar range, the number of anions (i.e., tetrafluoroborates) in the vicinity of the noncharged ferrocene species becomes small. To preserve the electro-neutrality upon electro-oxidation of Fc, therefore, extra work is required for migrating counterions to the generated ferrocenium cationes. This extra energy required for the electro-oxidation translates into considerable positive shifts in the anodic peak of the voltammograms. Upon the reverse sweep of the applied potential, a consequent reduction of the ferrocenium cation requires extra energy for removing the counterions away from the electrogenerated noncharged Fc species, causing a positive shift in the cathodic peak and overall a positive shift in the calculated  $E_{\text{Fc}^+/_{\text{Fc}}}^{(1/2)}$ .<sup>17</sup> Hence, the dilution of the supporting electrolyte adds an overpotential to the values of the measured half-wave potentials,  $E_{\text{Fc}^+/_{\text{Fc}}}^{(1/2)}$ , deviating them from the value of the “true” thermodynamic redox potential,  $E_{\text{Fc}^+/_{\text{Fc}}}^{(0)}$ .

Furthermore, the electrogeneration of ferrocenium, along with the attracted counterions, increases the local concentration of ions in the vicinity of the working electrode, decreasing the

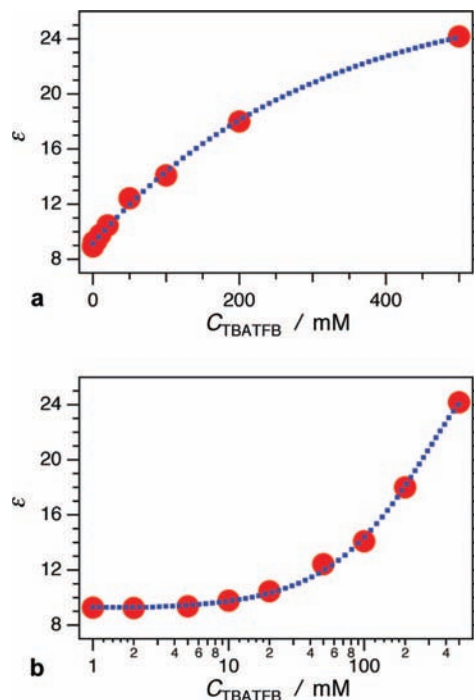


**Figure 5.** Dependence of the dielectric constant of the electrolyte solutions,  $\epsilon$ , on the electrolyte concentration,  $C_{\text{TBATFB}}$ , presented (a) linearly and (b) logarithmically. The values of  $\epsilon$  were obtained from the values of the fluorescence maxima (Figure 4b, c) and the calibration line in Figure 3b. The dotted lines represent an exponential fit of the dielectric constant vs the TBATFB concentration.

**TABLE 2: Dielectric Constants,  $\epsilon$ , of  $\text{CH}_2\text{Cl}_2$  Solutions Containing TBATFB with Different Concentrations<sup>a</sup>**

$C_{\text{TBATFB}}/\text{mM}$	$\epsilon$
0	8.93
1	9.23
2	9.26
5	9.36
10	9.77
20	10.5
50	12.4
100	14.1
200	18.0
500	24.2

<sup>a</sup> The dielectric constants are obtained from fluorescence data (Figures 3–5).

resistivity of the solution in that region. (Although this phenomenon is referred as “ohmic polarization,” it should be noted that in the presence of faradic current, the resistance is current-dependent, especially for diluted electrolyte solutions; i.e., the solution media in the vicinity of the working and counter electrodes does not obey Ohm’s law.<sup>17</sup>) Oldham quantified this effect of ohmic polarization, and later, other authors confirmed it:<sup>17–19</sup>

$$E_{\text{Fc}^+/_{\text{Fc}}}^{(1/2)} = E_{\text{Fc}^+/_{\text{Fc}}}^{(0)} + \frac{k_{\text{B}}T}{nq} \ln \left( \frac{D_{\text{Fc}}}{D_{\text{Fc}^+}} \left( 1 + \frac{D_{\text{Fc}} C_{\text{Fc}}}{D_{\text{Fc}^+} C_{\text{THATFB}}} \right) \right) \quad (4)$$

where  $D_{\text{Fc}}$  and  $D_{\text{Fc}^+}$  are the diffusion coefficients of the ferrocene and ferrocenium, respectively;  $C_{\text{Fc}}$  and  $C_{\text{TBATFB}}$  are the bulk concentrations of the ferrocene and of the electrolyte, respectively;  $k_{\text{B}}$  is the Boltzmann constant;  $T$  is the temperature;  $q$  is an elementary charge; and  $n$  is the number of electrons transferred from the ferrocene to the electrode.

A decrease in  $C_{\text{TBATFB}}$  from 10 to 1 mM produces up to 0.4 V shifts in  $E_{\text{Fc}^+/_{\text{Fc}}}^{(1/2)}$  (Figure 2). Equation 4, however, predicts such

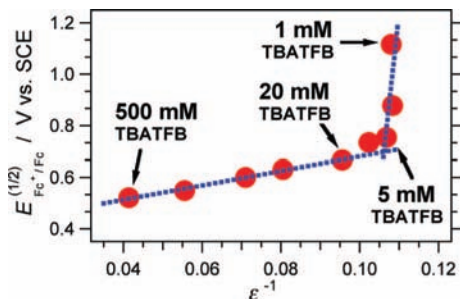


**Figure 6.** Correlation between the half-wave oxidation potential of ferrocene and the inverse dielectric constant of dichloromethane solutions with different concentrations of electrolyte, TBATFB. The correlation coefficient for the region between 20 and 500 mM TBATFB is 0.997.

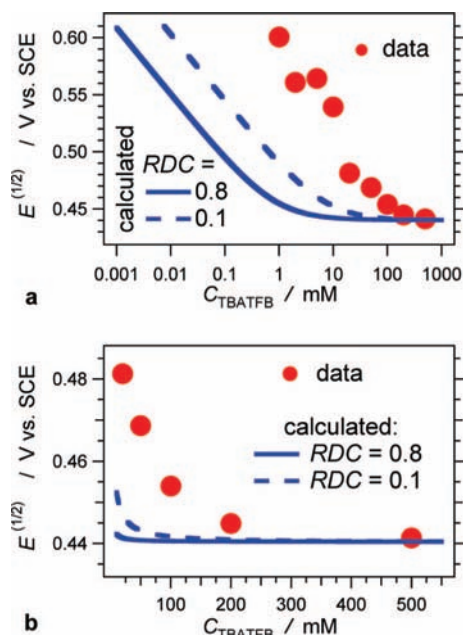


**Figure 7.** Comparison between the experimentally measured and the calculated (from eq 4) dependence of the half-wave potential of ferrocene,  $E_{\text{Fc}^+/\text{Fc}}^{(1/2)}$ , on the concentration of the supporting electrolyte,  $C_{\text{TBATFB}}$ , for acetonitrile. Calculated dependence for two diffusion coefficient ratios,  $\text{RDC} = D_{\text{Fc}^+}/D_{\text{Fc}}$ , and the measured values represented in (a) a logarithmic concentration scale, and (b) a linear concentration scale. The reported values for  $D_{\text{Fc}^+}$  and  $D_{\text{Fc}}$  in concentrated electrolyte solution in MeCN are about  $2.1 \times 10^{-5}$  and  $2.6 \times 10^{-5}$   $\text{cm}^2 \text{s}^{-1}$ , respectively, for which  $\text{RDC} = 0.8$ . The RDC value of 0.1 is hypothetical for demonstrating the dependence of  $E_{\text{Fc}^+/\text{Fc}}^{(1/2)}$  on  $C_{\text{TBATFB}}$ .

tenths-of-a-volt shifts only for  $C_{\text{Fc}}$  exceeding  $C_{\text{TBATFB}}$  at least 100 fold;<sup>17</sup> i.e., for electrolyte concentrations smaller than 50  $\mu\text{M}$  for 5 mM Fc solutions (Figure 7). As Pendley et al. pointed out, however, eq 4 implies two principal assumptions: (1) the rate of the heterogeneous electron transfer is relatively fast and does not depend on the electrolyte concentration; and (2) the ratio between the diffusion coefficients,  $\text{RDC} = D_{\text{Fc}^+}/D_{\text{Fc}}$ , does not depend on the electrolyte concentration.<sup>19</sup> The fast rates recorded for heterogeneous electron transfer for ferrocene<sup>12,13</sup> suggest that the first assumption is acceptable. Therefore, the concentration dependence of the diffusion coefficients may offer a plausible reason for the observed discrepancies at low electrolyte concentrations.

The diffusion coefficient is inversely proportional to the size of the species,  $r$ , and to the viscosity of the media,  $\eta$ ; from the Stokes–Einstein equation,  $D = k_{\text{B}}T/6\pi\eta r$ . Neither the solvent

( $\text{CH}_2\text{Cl}_2$ ) nor the electrolyte ions have a tendency for bonding with the noncharged ferrocene. Changes in the electrolyte concentration, therefore, should not change the effective size of the ferrocene ions. For a range of organic solvents, however, an increase in the concentration of the supporting electrolyte increases the viscosity of the solutions.<sup>20–22</sup> Therefore, a decrease in  $C_{\text{TBATFB}}$  can result in a substantial increase in the diffusion coefficient of ferrocene.<sup>22,23</sup> For ferrocenium ions in dilute solutions, on the other hand, the electrostatic effects can overcome the viscosity-induced modulation of their diffusion properties.<sup>22,24</sup> A decrease in  $C_{\text{TBATFB}}$  can impede the mass transport of the charged ferrocenium ions due to a lack of electrostatic screening in diluted electrolyte solutions. The corollary of these effects, indeed, will be a decrease in  $D_{\text{Fc}^+}/D_{\text{Fc}}$  with dilution of the supporting electrolyte. Such a decrease in the ratio between the diffusion coefficients, RDC, does make the shifts of  $E_{\text{Fc}^+/\text{Fc}}^{(1/2)}$ , predicted by eq 4, apparent at relatively high concentrations of the supporting electrolyte (Figure 7a).

For the calculation of  $E_{\text{Fc}^+/\text{Fc}}^{(1/2)}$ , using eq 4, we introduced constant values for the ratio  $D_{\text{Fc}^+}/D_{\text{Fc}}$ .<sup>25–27</sup> Although such calculations demonstrate the trends expected with the change in the diffusion coefficients, they do not reflect the dependence of RDC on the concentration of the supporting electrolyte; that is, for the calculations, the ratio  $D_{\text{Fc}^+}/D_{\text{Fc}}$  was assumed to be constant, rather than concentration-dependent, i.e.,  $D_{\text{Fc}^+}(C_{\text{TBATFB}})/D_{\text{Fc}}(C_{\text{TBATFB}})$ .

Another deficiency of eq 4 representing the relationship between  $E_{\text{Fc}^+/\text{Fc}}^{(1/2)}$  and  $E_{\text{Fc}^+/\text{Fc}}^{(0)}$  is the lack of a Born correction term for the change in the solvation energy due to the alteration in the dielectric constant of the solutions induced by the changes in the concentration of the supporting electrolyte. Examination of the calculated results from eq 4, however, shows a lack of concentration dependence of  $E_{\text{Fc}^+/\text{Fc}}^{(1/2)}$  at relatively large  $C_{\text{TBATFB}}$  (Figure 7b); that is, according to eq 4,  $E_{\text{Fc}^+/\text{Fc}}^{(0)} \approx E_{\text{Fc}^+/\text{Fc}}^{(1/2)}$  for  $C_{\text{Fc}} \ll C_{\text{TBATFB}}$ . The experimental data, however, do manifest a  $C_{\text{TBATFB}}$  dependence of  $E_{\text{Fc}^+/\text{Fc}}^{(1/2)}$ , even for  $C_{\text{TBATFB}} > 50$  mM. As it was discussed in the previous section, this dependence of  $E_{\text{Fc}^+/\text{Fc}}^{(1/2)}$  on  $C_{\text{TBATFB}}$  (i.e., of  $E_{\text{Fc}^+/\text{Fc}}^{(1/2)}$  on the dielectric constant of the media) can be readily quantified by using the Born relationship (Figure 6). Therefore, the “true” redox potentials,  $E_{\text{Fc}^+/\text{Fc}}^{(0)}$  (e.g., for neat solvents), can be readily extracted from the half-wave potentials,  $E_{\text{Fc}^+/\text{Fc}}^{(1/2)}$ , electrochemically measured at high concentrations of supporting electrolyte, by employing the Born dependence of the solvation energy on the dielectric constants of the solutions.

**Prediction of the Oxidation Potential of Ferrocene for Neat Solvents.** Using values of redox potentials,  $E_{\text{D}^{\text{ox}}/\text{D}^{\text{red}}}$  and  $E_{\text{A}^{\text{ox}}/\text{A}^{\text{red}}}$ , for the donor and the acceptor, respectively, in neat solvents in the Rehm–Weller equation (eq 1) will allow for the use of the dielectric constants of the corresponding neat solvent for  $\epsilon_{\text{D}}$  and  $\epsilon_{\text{A}}$  in the Born correction term (eq 2). The observed linear dependence of  $E_{\text{Fc}^+/\text{Fc}}^{(1/2)}$  on  $\epsilon^{-1}$  for  $\text{CH}_2\text{Cl}_2$  with high electrolyte concentration ( $20 \text{ mM} \leq C_{\text{TBATFB}} \leq 500 \text{ mM}$ ) allowed us to extrapolate the values for the oxidation potentials for neat solvents (Table 3, fourth column). The oxidation potentials for the neat solvents were extrapolated on the basis of the solvation energy of the electrogenerated ferrocenium cations and did not contain the overpotential introduced by long-range diffusion of counterions in diluted electrolyte solutions. Therefore, the extrapolated potentials had less-positive values than the values of  $E_{\text{Fc}^+/\text{Fc}}^{(1/2)}$  for some of the diluted electrolytes in the same solvents (Tables 1 and 3).

The extrapolation of redox potentials from the linear dependence of  $E_{\text{Fc}^+/\text{Fc}}^{(1/2)}$  on  $\epsilon^{-1}$  requires prior knowledge of the dielectric

**TABLE 3: Extrapolated Half-Wave Oxidation Potentials of Ferrocene,  $E_{\text{Fc}^+/ \text{Fc}}^{(1/2)}$ , for Neat Dichloromethane, Acetonitrile, and Dimethylformamide<sup>a</sup>**

solvent	$\epsilon$	$\epsilon^{-1}$	$E_{\text{Fc}^+/ \text{Fc}}^{(1/2) b}$	$E_{\text{Fc}^+/ \text{Fc}}^{(1/2) c}$
CH <sub>2</sub> Cl <sub>2</sub>	8.93	0.112	0.71	0.69
MeCN	36.6	0.0273	0.48	0.49
DMF	38.3	0.0261	0.47	0.45
super polar media <sup>d</sup>	$\infty$	0.000	0.40	

<sup>a</sup> The oxidation potentials are reported in volts vs SCE.

<sup>b</sup> Oxidation potentials for neat solvents obtained from the linear correlation between the measured half-wave potential and the inverse dielectric constant for electrolyte solutions, for the range between 20 and 500 mM TBATFB in CH<sub>2</sub>Cl<sub>2</sub> (Figure 6).

<sup>c</sup> Oxidation potentials for neat solvents obtained from the exponential relation between the half-wave potential and electrolyte concentration for the corresponding CH<sub>2</sub>Cl<sub>2</sub>, MeCN, and DMF solutions (Figure 7). <sup>d</sup> Media with high dielectric constant, for which  $\epsilon^{-1}$  can be approximated to zero.

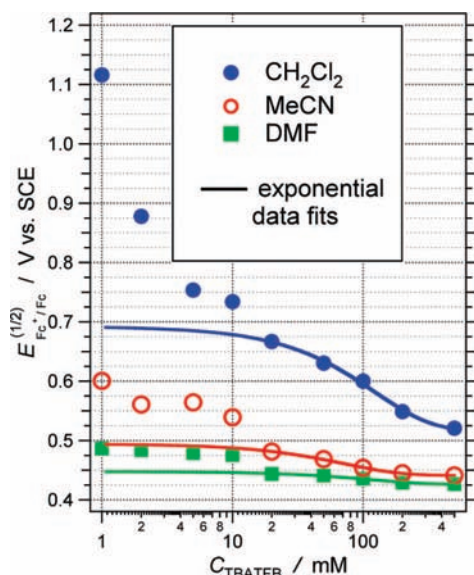


**Figure 8.** Dependence of the half-wave oxidation potential of ferrocene on the concentration of the supporting electrolyte. The exponential data fits were performed for the concentration region between 20 and 500 mM TBATFB.

constants of the corresponding electrolyte solutions with a broad range of concentrations. Using solvatochromism of fluorescent chromophores presents a facile approach for estimating the dielectric constants of electrolyte solutions. Chromophores that manifest large spectral fluorescence (or absorption) shifts in the dielectric range for electrolyte solutions of interests, however, might not be always readily available. Therefore, we examined an alternative approach for extrapolation of the oxidation potentials to zero electrolyte concentrations that requires solely electrochemical data.

Because of the exponential dependence of the measured dielectric constants on the electrolyte concentration (Figure 5), we predicted an exponential dependence of  $E_{\text{Fc}^+/ \text{Fc}}^{(1/2)}$  on  $C_{\text{TBATFB}}$ ,

$$E_{\text{Fc}^+/ \text{Fc}}^{(1/2)}(C_{\text{TBATFB}}) = E_{\infty} + E_{\Delta C} e^{\gamma C_{\text{TBATFB}}} \quad (5)$$

where  $E_{\infty}$  is the oxidation potential at large electrolyte concentration, and for neat solvents,  $E_{\text{Fc}^+/ \text{Fc}}^{(1/2)} = E_{\text{Fc}^+/ \text{Fc}}^{(1/2)}(0) = E_{\infty} + E_{\Delta C}$ ;  $\gamma$  is an empirical parameter. Fitting the data within the electrolyte concentration range between 20 and 500 mM to eq 5 (Figure 8), yielded values for  $E_{\text{Fc}^+/ \text{Fc}}^{(1/2)}(0)$  equal to 0.69, 0.49, and 0.45 V vs SCE for neat CH<sub>2</sub>Cl<sub>2</sub>, MeCN, and DMF, respectively. These values

differ by  $\sim 2\text{--}4\%$  from the values for the same neat solvents obtained from the linear dependence of  $E_{\text{Fc}^+/ \text{Fc}}^{(1/2)}$  on  $\epsilon^{-1}$  (Table 3), indicating that the linear (Figure 6) and the exponential (Figure 8) extrapolation methods allow for obtaining the redox potentials for zero-electrolyte concentration with equal reliability. The latter method involving exponential extrapolation, however, has a significant advantage: it does not require prior knowledge of the dielectric constants of the electrolyte solutions.

The typical working range of electrolyte concentrations in organic solvent for analytical electrochemistry is between about 100 and 200 mM. Comparison among the values of  $E_{\text{Fc}^+/ \text{Fc}}^{(1/2)}(0)$  for the three solvents with the corresponding measured values for  $C_{\text{TBATFB}} = 100$  and 200 mM (Table 1) reveals that the extrapolation of the oxidation potential to  $C_{\text{TBATFB}} = 0$  is not truly crucial for relatively polar solvents, such as MeCN and DMF. For both DMF and MeCN, the values of  $E_{\text{Fc}^+/ \text{Fc}}^{(1/2)}$  for 100 and 200 mM TBATFB are within a difference of 10% or less from the extrapolated values for the corresponding neat solvents.

For a relatively nonpolar solvent such as CH<sub>2</sub>Cl<sub>2</sub>, however, the extrapolation to  $C_{\text{TBATFB}} = 0$  mM proved to be important. The values of  $E_{\text{Fc}^+/ \text{Fc}}^{(1/2)}$  for 0, 100, 200, and 500 mM TBATFB in CH<sub>2</sub>Cl<sub>2</sub> are 0.69, 0.60, 0.55, and 0.52 V vs SCE, respectively (Figure 8 and Table 1). These values of  $E_{\text{Fc}^+/ \text{Fc}}^{(1/2)}$  reveal a considerable dependence of the redox potentials on the electrolyte concentration for relatively nonpolar solvents. For such solvents, therefore, extrapolation to zero electrolyte concentration may prove crucial for analyses of charge transfer processes, using eqs 1 and 2. For example, using the Born equation for calculating the values of the oxidation potential of Fc for DMF from the measured oxidation potentials for 100 and 200 mM electrolyte in CH<sub>2</sub>Cl<sub>2</sub> predicts  $E_{\text{Fc}^+/ \text{Fc}}^{(1/2)}(\text{DMF}) = 0.36$  and 0.31 V vs SCE, respectively. These predicted values considerably deviate from the determined value of 0.45 V vs SCE for  $E_{\text{Fc}^+/ \text{Fc}}^{(1/2)}(\text{DMF})$ . Alternatively, using the extrapolated value of 0.69 V vs SCE for neat CH<sub>2</sub>Cl<sub>2</sub> in the same calculations yields  $E_{\text{Fc}^+/ \text{Fc}}^{(1/2)}(\text{DMF}) = 0.45$  V vs SCE, which is in excellent agreement with the directly measured oxidation potential.

**Reduction Potential of Ph-ANI.** For a range of applications, dialkylamino-1,8-naphthalimides are acceptably good electron donors<sup>28–32</sup> and acceptors.<sup>33,34</sup> The cyclic voltammograms of Ph-ANI (Figure 3c) show an irreversible oxidation wave at about 1.1 V vs SCE and a reversible reduction wave at about  $-1.4$  V vs SCE (Figure 9a). We employed the exponential extrapolation analysis for determination of the half-wave reduction potential of Ph-ANI,  $E_{\text{ANI}/ \text{ANI}^{\cdot -}}^{(1/2)}$ , for neat acetonitrile.

As predicted by eqs 1 and 2, an increase in the media polarity shifts the oxidation potentials of noncharged species, such as ferrocene, toward less positive values (Figures 2 and 8) because the oxidized forms of the redox couples are charged. In contrast, an increase in the media polarity should shift the reduction potentials of noncharged species toward more positive values because the reduced forms of the redox couples are charged.

The values of  $E_{\text{ANI}/ \text{ANI}^{\cdot -}}^{(1/2)}$  determined from CV measurements of Ph-ANI for acetonitrile with different concentrations of TBATFB, indeed, showed the expected trend: the increase in the electrolyte concentration resulted in less negative values for  $E_{\text{ANI}/ \text{ANI}^{\cdot -}}^{(1/2)}$  (Figure 9b). Fitting the half-wave potential vs electrolyte concentration to an exponential function (Figure 9b) allowed us to extrapolate the reduction potential of Ph-ANI for neat acetonitrile; that is, for  $C_{\text{TBATFB}} = 0$  M and  $E_{\text{ANI}/ \text{ANI}^{\cdot -}}^{(1/2)} = -1.38 \pm 0.004$  V vs SCE.

**Implications for Charge-Transfer Studies.** We analyzed a hypothetical system in which ferrocene is an electron donor and Ph-ANI is an electron acceptor, separated 1 nm (center-to-center

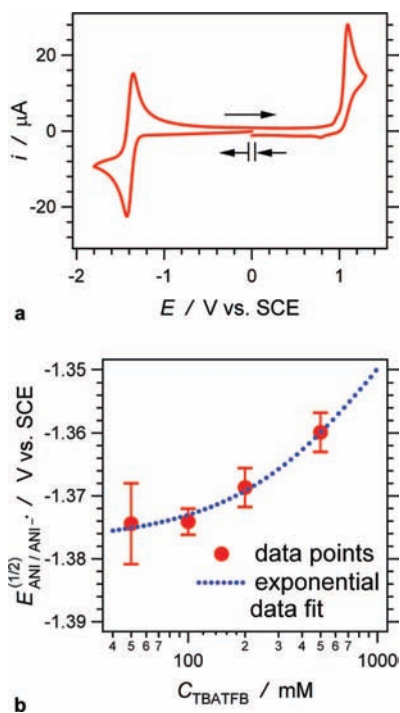


**Figure 9.** Electrochemical properties of Ph-ANI. (a) Cyclic voltammogram of Ph-ANI (5 mM) for acetonitrile in the presence of 100 mM TBATFB recorded at a scan rate of 50 mV/s. The arrows indicate the direction of the scan with the initial and the final point. (b) Dependence of the half-wave reduction potential of Ph-ANI for acetonitrile,  $E_{\text{ANI/ANI}^{-}}^{(1/2)}$ , on the electrolyte concentration,  $C_{\text{TBATFB}}$ , with a monoexponential data fit for extrapolation of the value of  $E_{\text{ANI/ANI}^{-}}^{(1/2)}$  for neat solvent; that is, for  $C_{\text{TBATFB}} = 0$ .

distance,  $R_{\text{DA}}$ , in eq 3) from each other. The half-wave redox potentials for acetonitrile (Figures 8 and 9) allowed us to estimate the energy of the charge-separated state,  $\Delta G_{\text{CS}}$ , of such a donor–acceptor system using eqs 1–3,  $\Delta G_{\text{CS}} = \Delta G_{\text{et}}^{(0)} + \mathcal{E}_{00}$ .

In the calculated values of  $\Delta G_{\text{CS}}$ , a discrepancy of about 0.04–0.07 eV became apparent when using data for redox potentials measured in the presence of 100–500 mM electrolyte solutions in comparison with  $\Delta G_{\text{CS}}$  calculated from redox potentials extrapolated to zero concentration for neat acetonitrile (Figure 10). Such errors, introduced by a direct use of redox potential measured for electrolyte solutions, can prove significant in the estimation of the driving force of photoinduced electron transfer,  $\Delta G_{\text{et}}^{(0)}$ , for cases when the energy of the charge-separated state,  $\Delta G_{\text{CS}}$ , is comparable to the photoexcitation zero-to-zero energy,  $\mathcal{E}_{00}$ .

Assuming Ph-ANI is the principal chromophore,  $\mathcal{E}_{00}$  varies between about 2.6 and 2.8 eV for media with different polarity, due to Ph-ANI solvatochromism. Therefore, for a relatively nonpolar media (e.g.,  $\epsilon$  between about 5 and 10),  $\Delta G_{\text{et}}^{(0)}$  will vary between about  $-0.2$  and  $0.2$  eV. A discrepancy of 0.04 eV, thus, will introduce an error of about 20% and more. Such discrepancy and errors will become significantly more pronounced for (1) large electrolyte concentrations; (2) low polarity of the solvents for the electrochemical measurements; and (3) small size of the redox species; that is, small  $r_{\text{D}}$  and  $r_{\text{A}}$  in eq 2.

Electrolyte solution media for electrochemical measurements should ideally be composed of relatively polar solvents. Instead of the solvent polarity, however, predominantly other factors, such as analyte solubility and electrochemical windows, govern the choices for solution media. For example, acetonitrile is a relatively polar solvent with a broad electrochemical window (spanning between about  $-2.5$  and  $2.5$  V vs SCE for 0.1 M

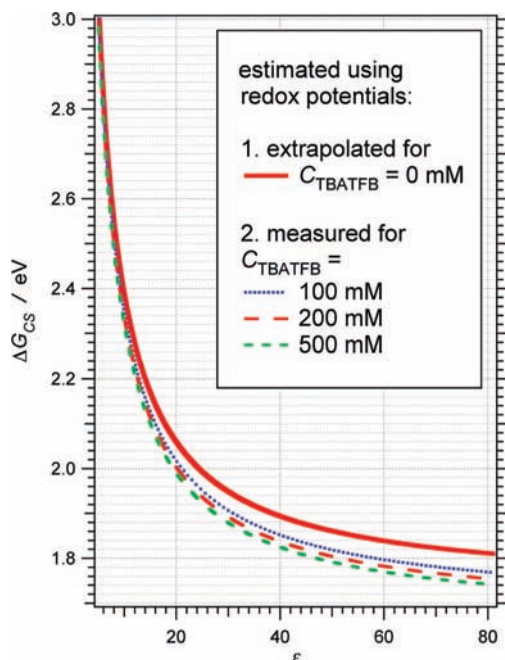


**Figure 10.** Dependence of the charge-separation energy,  $\Delta G_{\text{CS}}$ , on the dielectric constant of the media,  $\epsilon$ , calculated using eqs 1–3 for a charge-transfer system, in which ferrocene is an electron donor and Ph-ANI is an electron acceptor:  $\Delta G_{\text{CS}} = \Delta G_{\text{et}}^{(0)} + \mathcal{E}_{00}$ ;  $r_{\text{D}} = 2.6$  Å,  $r_{\text{A}} = 3.0$  Å, and  $R_{\text{DA}} = 10$  Å. For the oxidation potentials of  $E_{\text{D}^{\text{D}^{+n}}/\text{D}^{\text{D}}} \approx E_{\text{Fc}^{\text{+}}/\text{Fc}}$ , and for the reduction potential of the acceptor,  $E_{\text{A}^{\text{A}^{-n}}/\text{A}^{-n}} \approx E_{\text{ANI/ANI}^{-}}^{(1/2)}$ , we used the values of the half-wave potentials (1) measured for acetonitrile electrolyte solutions, 100, 200, and 500 mM TBATFB or (2) extrapolated to  $C_{\text{TBATFB}} = 0$  mM for neat acetonitrile. All  $\Delta G_{\text{CS}}\text{-vs-}\epsilon$  curves have the same shape. Because we adopted  $\epsilon_{\text{D}} = \epsilon_{\text{A}} = 36.6$  (i.e., for neat acetonitrile,  $C_{\text{TBATFB}} = 0$ ) for all calculations, the direct use of half-wave redox potentials in eq 1 for measurements for acetonitrile electrolyte solutions underestimates  $\Delta G_{\text{CS}}$  by about 0.04, 0.06, and 0.07 eV for 100, 200, and 500 mM TBATFB.

TBATFB),<sup>35</sup> and hence, it appears to be an excellent choice for redox measurements. Many large-molecular-weight organic conjugates, however, have a limited solubility in acetonitrile. Other solvents, such as benzonitrile or dichloromethane, which are less polar than acetonitrile and have narrower electrochemical windows, may offer the analyte solubility required for the redox measurements.<sup>36–38</sup>

DMF is a relatively polar solvent, but it is not the best choice for relatively extreme oxidation potentials because the electrochemical window for 0.1 M  $\text{Bu}_4\text{NClO}_4$  in DMF spans between about  $-2.7$  and  $1.5$  V vs SCE. Benzonitrile and dichloromethane (with 0.1 M TBATFB and  $\text{Bu}_4\text{NClO}_4$ , respectively), on the other hand, have electrochemical windows spanning from about  $-1.6$  to  $2.5$  V vs SCE and from about  $-1.9$  and  $1.7$  V vs SCE, respectively.<sup>35</sup>

A range of aprotic solvents, significantly less polar than acetonitrile and DMF, allow for shifting the electrochemical window. Ethers, such as tetrahydrofuran (THF), for example, allow for studying reduction processes at relatively extreme negative potentials (in addition to providing the required analyte solubility for the redox measurements).<sup>39–41</sup> For example, the electrochemical window for 0.1 M  $\text{Bu}_4\text{NClO}_4$  in THF spans between about  $-3$  and  $1.2$  V vs SCE.<sup>35,39</sup>

Nonpolar small-molecular-weight solvents tend to have relatively low viscosity. Therefore, for electrochemical studies requiring large diffusion rates and low-viscosity media, electrolyte solutions composed of nonpolar solvents, such as toluene, prove to be the choice.<sup>22</sup>

As we demonstrated for ferrocene–Ph-ANI donor–acceptor systems, neglecting the dependence of the measured redox potentials on the electrolyte concentration in acetonitrile can yield sensible errors in the estimation of relatively small driving forces,  $\Delta G_{\text{et}}^{(0)}$ , of photoinduced charge transfer (i.e., for cases, in which  $\Delta G_{\text{CS}}$  is comparable with  $\mathcal{E}_{00}$ ). Using relatively nonpolar solvents for electrochemical measurements further substantiates such errors in estimation of  $\Delta G_{\text{et}}^{(0)}$  that are induced by the dependence of the redox potentials on the concentration of the supporting electrolyte. For dichloromethane, for example, the difference between the measured (for  $C_{\text{TBATFB}} \geq 100$  mM) and extrapolated (to  $C_{\text{TBATFB}} = 0$  mM) values of the redox potentials can be 100 mV or more (Tables 1 and 3). For the donor and the acceptor, the effects of the electrolyte concentration on the oxidation and reduction potentials, respectively, manifest opposite trends (Figure 8 and 9), doubling the error in estimation of  $\Delta G_{\text{et}}^{(0)}$  to 0.2 eV or larger. Using values of redox potentials that are extrapolated to zero electrolyte concentration (Figure 8 and 9) offers an approach for eliminating such errors in the estimations of the driving force for charge-transfer processes.

## Conclusions

The dependence of the redox potentials on the concentration of the supporting electrolyte is considerably more pronounced for solutions composed of relatively nonpolar solvents (such as dichloromethane) than for solutions of relatively polar solvents (such as acetonitrile and dimethylformamide). Therefore, for redox measurements conducted with relatively polar solvents, approximating the dielectric constants,  $\epsilon_{\text{D}}$  and  $\epsilon_{\text{A}}$  (eq 2), with the values of the dielectric constants for the corresponding neat solvent will not result in considerable error in the estimation of relatively large charge-transfer driving forces; that is, for  $\Delta G_{\text{et}}^{(0)}$  exceeding about 0.5 eV. For a relatively small  $\Delta G_{\text{et}}^{(0)}$  and for electrochemical measurements involving relatively nonpolar solvents, such as dichloromethane, chloroform, and tetrahydrofuran, however, the values of the redox potentials (recorded at several different electrolyte concentrations) should be extrapolated to zero concentration prior to their use in the Rehm–Weller equation (eq 1). Such extrapolation will permit the use of the values of the dielectric constants of the corresponding neat solvents for  $\epsilon_{\text{D}}$  and  $\epsilon_{\text{A}}$  (eq 2). We believe that the described zero-concentration extrapolation method will extend the applicability of the Born term in the Rehm–Weller equation to electrochemical media composed of relatively nonpolar solvents and to cases involving a relatively small  $\Delta G_{\text{et}}^{(0)}$ .

## Experimental

**Materials.** Ferrocene, tetrabutylammonium tetrafluoroborate, 4-bromo-1,8-naphthalic anhydride, 3-dimethylaminopropanenitrile, 1,2-dimethoxyethane, acetic acid, and aniline were purchased from Aldrich. Anhydrous solvents (dichloromethane, acetonitrile, and *N,N*-dimethylformamide) and spectroscopic-grade solvents (chloroform, dichloromethane, benzonitrile, acetonitrile, and dimethylsulfoxide) were purchased from Fisher Scientific.

*N*-Phenyl-4-dimethylamino-1,8-naphthalimide (Ph-ANI) was prepared using a two-step synthesis by adopting published procedures.<sup>42,43</sup>

**4-Dimethylamino-1,8-naphthalic Anhydride.** 4-Bromo-1,8-naphthalic anhydride (1.0 g, 3.5 mmol) was suspended in 4 mL of 3-dimethylaminopropanenitrile, purged with argon, and heated to reflux. The solid material completely dissolved, forming a reddish-brown homogeneous solution. After three

hours, the reaction solution was allowed to cool to room temperature, forming a yellow precipitate. The precipitate was collected by filtration, washed with Milli-Q water and ethanol, and dried under vacuum at elevated temperature to produce an orange solid, 4-dimethylamino-1,8-naphthalic anhydride (0.52 g, 60% yield). <sup>1</sup>H NMR (300 MHz, DMSO-*d*<sub>6</sub>),  $\delta$ /ppm: 8.60 (d, 1H), 8.47 (d, 1H), 8.34 (d, 1H), 7.77 (t, 1H), 7.21 (d, 1H), 3.17 (s, 6H).

***N*-Phenyl-4-dimethylamino-1,8-naphthalimide (Ph-ANI).** 4-Dimethylamino-1,8-naphthalic anhydride (150 mg, 0.62 mmol) was mixed with 0.34 mL of aniline (~3.6 mmol) in 3 mL of 1,2-dimethoxyethane. The reaction mixture was purged with argon and heated to 90 °C. When the reflux began, 1 mL of acetic acid was added to the mixture. After 12 h of reflux, the reaction was allowed to cool to room temperature. The cooled mixture was diluted with 200 mL of water, and the fine precipitate that formed was allowed to coagulate for 12 h. The precipitate was collected by filtration, washed with Milli-Q water and ethanol, and dried under vacuum at elevated temperature to produce an orange-yellow solid, Ph-ANI, with high purity (0.11 g, 57% yield). (The purity of the product was tested with TLC and HPLC.) <sup>1</sup>H NMR (300 MHz, DMSO-*d*<sub>6</sub>),  $\delta$ /ppm: 8.56 (d, 1H), 8.42 (d, 1H), 8.36 (d, 1H), 7.80 (t, 1H), 7.50 (m, 3H), 7.34 (d, 2H), 7.23 (d, 1H), 3.11 (s, 6H).

**Cyclic Voltammetry.** The electrochemical measurements were conducted at ambient room temperature (~20 °C) using a Reference 600 potentiostat-galvanostat (Gamry Instruments, Warminster, PA), equipped with a three-electrode cell. Glassy carbon electrode and platinum wire were used for the working and counter electrodes, respectively. A saturated calomel electrode (Gamry Instruments) was used for a reference electrode. To prevent contamination, the reference electrode was brought in contact with the sample solutions via two salt bridges. When not in use, the reference electrode was stored submerged in saturated potassium chloride solution. For all samples, the ferrocene concentration was 5 mM. For each sample, at least five scans were recorded at scan rates between 0.1 and 0.5 V/min.

**Fluorescence Measurements.** Steady-state emission measurements were conducted with a FluoroLog-3 spectrofluorometer (Horiba-Jobin-Yvon) equipped with double-grating monochromators and a TBX single-photon-counting detector. By adjusting the slit widths, the signal at all wavelengths was kept under 10<sup>6</sup> CPS to ensure that it was within the linear range of the detector. Concurrently, the intensity of the excitation light was also monitored at a reference detector. At each data point (1 point/nm), the fluorescence intensity (recorded at the signal detector) was divided by the excitation intensity (recorded at the reference detector) to correct the spectra for fluctuations in the intensity of the excitation source during the measurements. For all samples, the concentration of Ph-ANI was 10  $\mu$ M.

**Data Analysis.** The values for the peak maxima (and minima) from the cyclic voltammograms and from the fluorescence spectra were obtained by fitting the region around the maxima (or the minima) to a Gaussian function. The quality of the fits was monitored by examination of the residuals. All least-squares data fits were conducted using Igor Pro, version 6 (Wavemetrics, Inc.) on MacOS and Windows XP workstations. For each of the cyclic voltammograms, the half-wave potentials were obtained by averaging the potentials of the cathodic and the anodic peaks. For each set of conditions, at least five measurements were conducted. The error limits (Table 1) represent the standard deviation obtained for the corresponding set of measurements.



**Acknowledgment.** The funding for this work was provided by the UC Energy Institute. The support for B. Steyer, A. Gerasimenko, and A. Ferreira was provided by the National Science Foundation (EEC 0649096). The support for A. Contreras was also provided by the National Science Foundation (DBI 0731660).

## References and Notes

- (1) Rehm, D.; Weller, A. *Isr. J. Chem.* **1970**, *8*, 259–271.
- (2) Verhoeven, J. W.; van Ramesdonk, H. J.; Groeneveld, M. M.; Benniston, A. C.; Harriman, A. *ChemPhysChem* **2005**, *6*, 2251–2260.
- (3) Braslavsky, S. E.; Acuna, A. U.; Adam, W.; Amat, F.; Armesto, D.; Atvars, T. D. Z.; Bard, A.; Bill, E.; Bjoern, L. O.; Bohne, C.; Bolton, J.; Bonneau, R.; Bouas-Laurent, H.; Braun, A. M.; Dale, R.; Dill, K.; Doepp, D.; Duerr, H.; Fox, M. A.; Gandolfi, T.; Grabowski, Z. R.; Griesbeck, A.; Kutateladze, A.; Litter, M.; Lorimer, J.; Mattay, J.; Michl, J.; Miller, R. J. D.; Moggi, L.; Monti, S.; Nonell, S.; Ogilby, P.; Olbrich, G.; Oliveros, E.; Olivucci, M.; Orellana, G.; Prokorenko, V.; Naqvi, K. R.; Rettig, W.; Rizzi, A.; Rossi, R. A.; San Roman, E.; Scandola, F.; Schneider, S.; Thulstrup, E. W.; Valeur, B.; Verhoeven, J.; Warman, J.; Weiss, R.; Wirz, J.; Zachariasse, K. *Pure Appl. Chem.* **2007**, *79*, 293–465.
- (4) Born, M. Z. *Phys.* **1920**, *1*, 45–48.
- (5) Rashin, A. A.; Honig, B. *Ann. N.Y. Acad. Sci.* **1986**, *482*, 143–144.
- (6) Oseki, Y.; Fujitsuka, M.; Cho, D. W.; Sugimoto, A.; Tojo, S.; Majima, T. *J. Phys. Chem. B* **2005**, *109*, 19257–19262.
- (7) Tavernier, H. L.; Kalashnikov, M. M.; Fayer, M. D. *J. Chem. Phys.* **2000**, *113*, 10191–10201.
- (8) Wan, J.; Ferreira, A.; Xia, W.; Chow, C. H.; Takechi, K.; Kamat, P. V.; Jones, G.; Vullev, V. I. *J. Photochem. Photobiol., A* **2008**, *197*, 364–374.
- (9) Zhang, J.; Bond, A. M. *Analyst* **2005**, *130*, 1132–1147.
- (10) Rogers, E. I.; Silvester, D. S.; Poole, D. L.; Aldous, L.; Hardacre, C.; Compton, R. G. *J. Phys. Chem. C* **2008**, *112*, 2729–2735.
- (11) Gritzner, G. *Pure Appl. Chem.* **1990**, *62*, 1839–1858.
- (12) Bond, A. M.; Henderson, T. L. E.; Mann, D. R.; Mann, T. F.; Thormann, W.; Zoski, C. G. *Anal. Chem.* **1988**, *60*, 1878–1882.
- (13) Montenegro, M. I.; Pletcher, D. J. *Electroanal. Chem. Interfacial Electrochem.* **1986**, *200*, 371–374.
- (14) Tsierkezos, N. G. *J. Solution Chem.* **2007**, *36*, 289–302.
- (15) Abeed, F. A.; Al-Allaf, T. A. K.; Sulaiman, S. T. *Analyst* **1988**, *113*, 333–336.
- (16) Bond, A. M.; McLennan, E. A.; Stojanovic, R. S.; Thomas, F. G. *Anal. Chem.* **1987**, *59*, 2853–2860.
- (17) Oldham, K. B. *J. Electroanal. Chem. Interfacial Electrochem.* **1988**, *250*, 1–21.
- (18) Drew, S. M.; Wightman, R. M.; Amatore, C. A. *J. Electroanal. Chem. Interfacial Electrochem.* **1991**, *317*, 117–124.
- (19) Pendley, B. D.; Abruna, H. D.; Norton, J. D.; Benson, W. E.; White, H. S. *Anal. Chem.* **1991**, *63*, 2766–2771.
- (20) Casteel, J. F.; Angel, J. R.; McNeeley, H. B.; Sears, P. G. *J. Electrochem. Soc.* **1975**, *122*, 319–324.
- (21) Rebagay, T. V.; Casteel, J. F.; Sears, P. G. *J. Electrochem. Soc.* **1974**, *121*, 977–982.
- (22) Bento, M. F.; Geraldo, M. D.; Montenegro, M. I. *Anal. Chim. Acta* **1999**, *385*, 365–371.
- (23) Zhou, H.; Dong, S. *Electrochim. Acta* **1997**, *42*, 1801–1807.
- (24) Dong, S.; Zhou, H. *J. Electroanal. Chem.* **1996**, *403*, 117–123.
- (25) Martin, R. D.; Unwin, P. R. *Anal. Chem.* **1998**, *70*, 276–284.
- (26) Ikeuchi, H.; Kanakubo, M. *Electrochemistry (Tokyo)* **2001**, *69*, 34–36.
- (27) Jacob, S. R.; Hong, Q.; Coles, B. A.; Compton, R. G. *J. Phys. Chem. B* **1999**, *103*, 2963–2969.
- (28) Lockard, J. V.; Wasielewski, M. R. *J. Phys. Chem. B* **2007**, *111*, 11638–11641.
- (29) Chernick, E. T.; Mi, Q.; Vega, A. M.; Lockard, J. V.; Ratner, M. A.; Wasielewski, M. R. *J. Phys. Chem. B* **2007**, *111*, 6728–6737.
- (30) Chernick, E. T.; Mi, Q.; Kelley, R. F.; Weiss, E. A.; Jones, B. A.; Marks, T. J.; Ratner, M. A.; Wasielewski, M. R. *J. Am. Chem. Soc.* **2006**, *128*, 4356–4364.
- (31) Keinan, S.; Ratner, M. A.; Marks, T. J. *Chem. Phys. Lett.* **2006**, *417*, 293–296.
- (32) Sinks, L. E.; Weiss, E. A.; Giaimo, J. M.; Wasielewski, M. R. *Chem. Phys. Lett.* **2005**, *404*, 244–249.
- (33) Veale, E. B.; Gunnlaugsson, T. *J. Org. Chem.* **2008**, *73*, 8073–8076.
- (34) Grabchev, I.; Dumas, S.; Chovelon, J.-M.; Nedelcheva, A. *Tetrahedron* **2008**, *64*, 2113–2119.
- (35) Bard, A. J.; Faulkner, L. R. *Electrochemical Methods: Fundamentals and Applications*, 2nd ed.; John Wiley & Sons, Inc.: New York, 2001.
- (36) Kanato, H.; Takimiya, K.; Otsubo, T.; Aso, Y.; Nakamura, T.; Araki, Y.; Ito, O. *J. Org. Chem.* **2004**, *69*, 7183–7189.
- (37) van Haare, J. A. E. H.; Groenendaal, L.; Peerlings, H. W. I.; Havinga, E. E.; Vekemans, J. A. J. M.; Janssen, R. A. J.; Meijer, E. W. *Chem. Mater.* **1995**, *7*, 1984–1989.
- (38) Kumagai, A.; Fukumoto, H.; Yamamoto, T. *J. Phys. Chem. B* **2007**, *111*, 8020–8026.
- (39) Bennett, B. L.; Robins, K. A.; Tennant, R.; Elwell, K.; Ferri, F.; Bashta, I.; Aguinado, G. *J. Fluorine Chem.* **2006**, *127*, 140–145.
- (40) Paolucci, F.; Carano, M.; Ceroni, P.; Mottier, L.; Roffia, S. *J. Electrochem. Soc.* **1999**, *146*, 3357–3360.
- (41) Paddon, C. A.; Bhatti, F. L.; Donohoe, T. J.; Compton, R. G. *J. Phys. Org. Chem.* **2007**, *20*, 115–121.
- (42) Plakidin, V. L.; Vostrova, V. N. *Zh. Org. Khim.* **1983**, *19*, 2591–2600.
- (43) Plakidin, V. L.; Vostrova, V. N. *Zh. Org. Khim.* **1981**, *17*, 1118–1119.

JP809105F